Absolute cross-section measurements for electron-impact ionization of Cl^+

N. Djurić,* E. W. Bell, E. Daniel,† and G. H. Dunn‡
Joint Institute for Laboratory Astrophysics, University of Colorado and National Institute of Standards and Technology, Boulder, Colorado 80309-0440
(Received 5 February 1992)

Absolute cross sections for electron-impact ionization of Cl^+ have been measured from threshold to 200 eV with the use of the crossed-beams technique. The cross section shows a peak value of 12.8×10^{-17} cm^2 at about 70 eV. Results are compared to the semiempirical prediction formula of Lotz, with scaled cross sections for ions in the same isoelectronic sequence, and with other recent measurements. Expansion coefficients and formulas for generating ionization rate coefficients in the electron temperature range $10^4 \le T \le 10^7$ K are presented.

PACS number(s): 34.80.Kw

INTRODUCTION

Electron-impact ionization of positive ions is a fundamental process in many discharges or high-temperature stellar or fusion plasmas and has long been studied experimentally [1] and theoretically [2]. Total ionization cross sections are necessary data in modeling and understanding the various environments. Systematic studies, such as those along isoelectronic sequences, provide some generalization of aspects associated with atomic structure and are required for further theory development and predictor formulas.

In spite of the importance of ionization studies and the long history of study, particularly for controlled-fusion research [3], information is lacking. For instance, the only other ion isoelectronic with sulfur (sulfurlike) for which ionization cross sections have been measured is Ar^{2+} [4]. Chlorine is frequently found as an impurity in fusion devices, and in this paper we present experimental data on electron-impact ionization of another member of the sulfur sequence, Cl^+. The results are compared with other recent measurements [5].

EXPERIMENTAL METHOD

These measurements were performed using the crossed-beams technique. The apparatus is shown in Fig. 1 and the technique used has been described previously [6].

The ions are produced in a commercial hot cathode-discharge ion source [7] fed by CCl_4 gas. They are extracted through a hole in the molybdenum anode covered with a platinum foil disk (to extend the anode lifetime, since chlorine attacks the molybdenum) and accelerated to 4 keV. The Cl^+ component is mass selected by a 60° sector magnet and directed to a collision chamber in which the vacuum was maintained at approximately 5×10^{-8} Pa. After colliding with the electrons, the ions enter a parallel-plate electrostatic analyzer which separates the product doubly charged ions from the singly charged primary beam. The parent-ion-beam current is measured by collecting it in a Faraday cup, biased to suppress the loss of secondary electrons. When the parent beam is deflected into the Faraday cup, product ions are deflected to an electron multiplier [8] used to count individual ions. In front of the electrostatic analyzer is a set of vertical deflection plates, mounted to compensate for the ion-beam deflection in the 0.02 T magnetic field of the magnetically confined electron gun. The electron gun is almost identical to that described by Taylor and Dunn [9,10] and has been used in this laboratory for several earlier experiments. The electron-beam current was measured by collecting it in a suppressed collector designed to minimize the number of electrons reflected back along the magnetic-field lines into the collision region. The electron beam is chopped and the detector gated to detect counts with electrons on and electrons off, so that detector counts due to electron-impact ionization could be separated from background counts. A scanning slit probe located in the collision volume can be rotated to measure separately the spatial profiles of both the electron and the ion beams.

The absolute cross section σ at each energy E is determined from the signal count rate R of doubly charged ions, beam currents I_i and I_e of ions and electrons, elementary charge e, velocities v_i and v_e of the particles, form factor F (which takes the spatial overlap of the two beams into account), and detection efficiency ϵ for the product doubly charged ions, through the relationship [1,11]

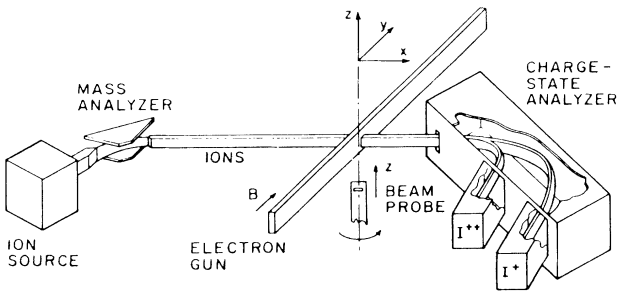

FIG. 1. Schematic of experiment.

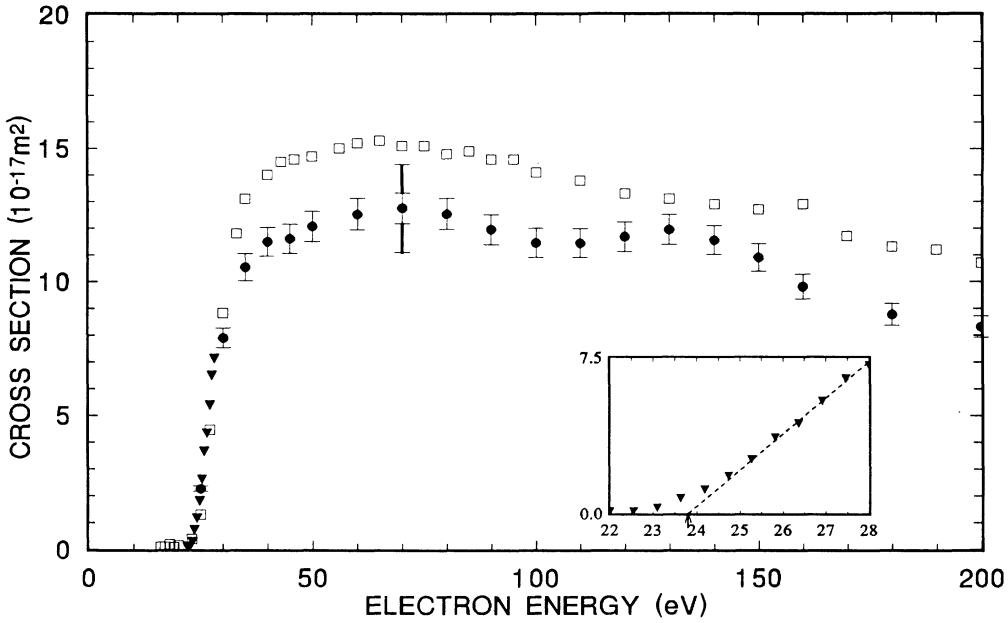

FIG. 2. Electron-impact-ionization cross section of Cl^+ vs electron energy. Inset shows the near-threshold region (▼). These are relative measurements of cross sections taken by scanning the electron energies over the chosen interval and are made absolute by normalization to the point at 25 eV. ●, present absolute measurements; □, absolute measurements from Ref. [5]. Relative uncertainties are shown for the present data as solid bars, while the absolute uncertainty is shown at 70 eV by the bold bar.

$$\sigma = \frac{Re^2}{I_e I_i} \frac{v_i v_e}{(v_i^2 + v_e^2)^{1/2}} \frac{F}{\epsilon} . \quad (1)$$

Typically, data were obtained using computer control to measure the beam distributions and to record signal and incident beam currents. Systematic checks and diagnostics were made [12–14] to verify that the quantities in Eq. (1) were measured correctly and that no extraneous effects gave misleading results.

The electron-energy scale was calibrated using a linear extrapolation method. The cross section rises approximately linearly for about the first 5 eV above threshold (see the inset of Fig. 2), and the very low signal below 23 eV illustrates that the number of metastable target ions is small and direct ionization from the ground state is the dominant process. Thus, by extrapolating the signal (apparent cross section) at low energy to the abscissa, one may equate the intercept with the known spectroscopic threshold value of 23.8 eV [15] for Cl^+.

Special care was taken with the pulse-counting circuitry and the measurement of the detection efficiency for the product ions. The secondary-electron multiplier [8] is a 20-stage focused dynode multiplier with a large sensitive area but less than unit efficiency. The detector was used in the pulse-counting mode, with negative high voltage (3650 V) applied to the first dynode and with the anode at ground potential. The energetic positive ions strike the surface of the first dynode generating secondary electrons, a process which depends on ion energy and charge state, angle of incidence, and previous history of the particular dynode surface. Resultant charge pulses are fed into a preamplifier, amplifier, and to a single-channel analyzer (SCA) for further amplification, discrimination, and standardization. The 0.5-μs dead time of the pulse-counting system typically led to corrections of 0.5% or less, and these corrections were made. By releasing more electrons per ion at the multiplier anode, the energetic doubly charged ions could lead to saturation of the amplifiers, and so pulse shapes were often checked for distortion at different points of circuitry.

In addition, the pulse-height distribution (PHD) also varies with ion-impact energy. The variation of detection efficiency as well as PHD's with ion-impact energy can lead to systematic errors in measuring signal rates by pulse counting. Integral pulse-height distributions were measured at different high voltages applied to the multiplier as a function of discriminator level, allowing the proper setting of the lower threshold of a SCA to be determined. After all these preliminary tests have been done, one can proceed with the experiment on electron-impact ionization and on detector-efficiency measurements.

The detector efficiency for the product Cl^{2+} ions was determined in a separate experiment. A beam of Cl^{2+} ions of kinetic energy equal to that of the product ions in the experiment (2×2000 eV) was produced from the ion source with a current of about 1×10^{-14} A or less. The beam current I_{2+} was measured by adjusting the analyzer to direct the Cl^{2+} ions into the primary ion Faraday cup which was connected to a calibrated and sensitive, vibrating-reed electrometer [16]. The ion beam was then directed onto the electron multiplier detector by adjusting the analyzer voltage, and the pulse rate R was

measured. The efficiency was then determined simply from $\epsilon = 2e\Delta R / \Delta I_{2+}$, where the respective Δ's are rate and current differences when the beam is on or off. A series of independent measurements at different times over the period of the experiment yielded a detection efficiency of 0.491 ± 0.002.

RESULTS

The measured cross sections for electron-impact ionization of Cl^{2+} are listed in Table I and shown in Fig. 2. The solid circles in Fig. 2 are independent absolute measurements of the cross section measured at each energy, and they represent weighted averages of results from repeated data runs. Form factors were measured at each energy in all data runs. Uncertainties shown are relative uncertainties at the 90% confidence level (CL), except for the point at 70 eV which also shows the $\pm 10\%$ high confidence level (estimated at roughly equivalent to 90% CL) absolute uncertainty. Solid triangles are relative measurements in the threshold region normalized to the absolute measurement at 25 eV.

Also shown as open squares in Fig. 2 are the measurements of Yamada *et al.* [5]. Over much of the energy range, the two measurements are disparate by around 25%. This is outside the range assessed for either of the two experiments. In looking for possible differences in technique which could account for the discrepancy, we note that apparently Yamada *et al.* calibrated their detector using various noble-gas ions and assumed that the calibration holds for other ions. In so doing, they noted constancy of efficiency for the noble-gas ions measured and pointed to a similarity between the efficiency and the ratio of geometric channel area to total area of the microchannel plate detector they used. They also measured the ionization of Ar^+ and obtained good agreement with results of Müller *et al.* [17] and Mann, Smith, and Harrison [18]. In a similar manner, we also measured the ionization of Ar^+ and found good agreement with these authors.

TABLE I. Absolute cross sections for electron-impact ionization of Cl^+ obtained as weighted averages of results from repeated data runs. Cross-section uncertainties are relative only and are at the 90% confidence level (CL). Additionally, there are systematic uncertainties leading to an additional absolute uncertainty of $\pm 10\%$ at high CL (estimated equivalent to 90% CL).

E (eV)	σ (10^{-17} cm^2)	E (eV)	σ (10^{-17} cm^2)
25	2.3±0.1	100	11.5±0.5
30	7.9±0.4	110	11.4±0.5
35	10.5±0.5	120	11.7±0.6
40	11.5±0.5	130	11.9±0.6
45	11.6±0.6	140	11.6±0.5
50	12.1±0.6	150	10.9±0.5
60	12.5±0.6	160	9.8±0.5
70	12.8±0.6	180	8.8±0.4
80	12.5±0.6	200	8.3±0.4
90	11.9±0.6		

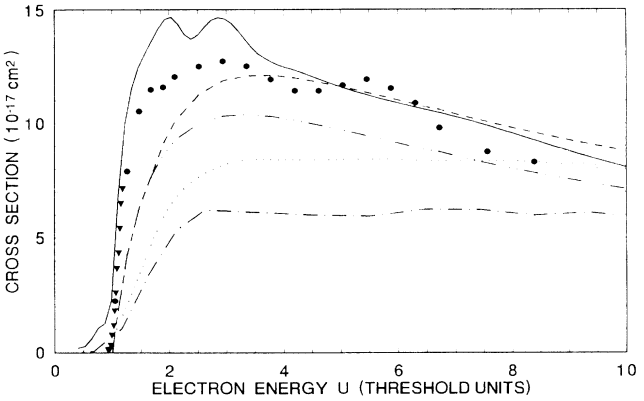

FIG. 3. Ionization cross sections scaled [Eq. (2)] to that for Cl^+ vs reduced electron energy $u = E/E_I$ for Ar^{2+}: ——, Ref. [4]; Cl^+: ▼ and ●, present data as in Fig. 2; S: —·—·—·, Ref. [20], · · · ·, Ref. [21]; - · · · -, the prediction from the Lotz formula with coefficient values for the $3p$ subshell only and — — —, including $3s3p$ subshells.

In Fig. 3 our measured results for Cl^+ are compared with scaled cross sections for other isoelectronic targets (Ar^{2+}, S) and with predictions of the Lotz [19] semiempirical formula for the direct-ionization cross section. Cross sections for Ar^{2+} are from Ref. [4] and those for S are from Refs. [20] and [21]. We note that in the absence of measurements on Cl^+, Lennon *et al.* [22] in their compendium recommend a curve based upon smoothed Ar^{2+} cross sections to represent the cross sections for Cl^+. In Fig. 3 we have chosen to scale the cross sections of isoelectronic species *relative to that for* Cl^+ using the classical scaling law

$$\sigma_s(u) = \left[\frac{E_I}{23.8} \right]^2 \sigma(u) \ . \tag{2}$$

Here $u = E/E_I$, E is the energy of the incident electron, E_I is the threshold ionization energy of the subject target, 23.8 eV is the ionization energy of Cl^+, and $\sigma(u)$ is the ionization cross section for the subject target as a function of electron energy in threshold units.

Comparison with the prediction of the Lotz formula is of interest, since this formula is heavily relied upon by various authors and user groups. The formula has been applied by using coefficient values originally recommended by Lotz [19] and subshell ionization energies given by Clementi and Roetti [23]. Curves including only the $3p$ subshell and including both the $3p$ and $3s$ subshells are shown. The rise of the measured cross section from threshold to 40–50 eV is steeper than that predicted by the Lotz formula, and one can attempt to attribute the difference to indirect processes (e.g., excitation of inner-shell $3s$ electrons to autoionizing states). Structure that appears near 120 eV is similar to a feature in its isoelectronic neighbors Ar^{2+} [4] and S [20]. In the scaled Ar^{2+} the minimum appears near 70 eV ($u = 3$) and is quite narrow, in Cl^+ it is near 100 eV ($u = 4$) and is broader, while in scaled S the structure is much broader and the

TABLE II. Rate coefficients for ionization of Cl^+. Numbers in brackets signify factors of powers of 10.

T_e (K)	$\alpha(T)$ (cm^3/s)	T_e (K)	$\alpha(T)$ (cm^3/s)
1.0[+4]	2.91[−20]	6.0[+5]	4.74[−8]
2.0[+4]	3.81[−14]	8.0[+5]	5.33[−8]
4.0[+4]	4.80[−11]	1.0[+6]	5.66[−8]
6.0[+4]	5.35[−10]	2.0[+6]	5.98[−8]
8.0[+4]	1.81[−9]	4.0[+6]	5.54[−8]
1.0[+5]	3.77[−9]	6.0[+6]	5.11[−8]
2.0[+5]	1.68[−8]	8.0[+6]	4.77[−8]
4.0[+5]	3.67[−8]	1.0[+7]	4.50[−8]

minimum appears near 120 eV ($u=5$).

A principal goal of the present study was determination of absolute ionization cross sections. Thus no effort was made to measure cross sections in detail near structure. Nevertheless, the double-humped structure referred to was very reproducible in both the Cl^+ and the Ar^{2+} data, and appears plausible in the S data. We have no models or suggested explanations for this structure nor for the apparently regular progression of energies at which it appears. There is some evidence for the double-humped structure in the data of Yamada *et al.* [5], but it appears at a higher energy. One also observes that the slopes near threshold of the scaled cross sections are greater for the ions than for the neutral atoms. This behavior within an isoelectronic sequence is frequently—though not universally—observed [22], and at present we do not have, nor are we aware of, an explanation. It is clear that further theoretical work is needed to reach a better description of ionization cross sections for many-electron systems.

It is often necessary to know the rate coefficient as a function of electron temperature for ionization of an ion by electron impact. The rate coefficients are evaluated by integrating the product of cross section and velocity over a Maxwellian distribution following the procedure discussed by Crandall *et al.* [24]. The cross section data are fit with a cubic spline or piecewise cubic Hermite polynomial and extrapolated with relevant functional forms for lower and higher energies than measured. The convolution can then be performed in a piecewise analytic way over the $n-1$ data intervals and the extended regions to yield the rate coefficients. Some representative rate coefficients for Cl^+ are listed in Table II. To make it convenient to obtain coefficients at any temperature $10^4 \le T \le 10^7$ K, the coefficient data were fit with a Chebyshev expansion, and the expansion coefficients are presented in Table III. At any temperature in the above interval, $\alpha(T)$ can be obtained (here in units cm^3/s) by evaluating the expansion

TABLE III. Expansion coefficients for generating ionization rate coefficients using Eq. (3) or Eq. (4) for the interval $10^4 \le T \le 10^7$ K. Numbers in brackets signify factors of powers of 10.

a_0	2.820 301[−10]	a_5	5.184 646[−13]
a_1	−1.464 081[−10]	a_6	2.355 628[−13]
a_2	1.149 782[−11]	a_7	−4.712 102[−13]
a_3	1.079 981[−11]	a_8	7.210 388[−14]
a_4	−2.626 140[−12]		

$$\alpha(T)=e^{-I/kT}T^{1/2}\sum_{r=1}^{n}a_r T_r(X), \quad X=\left[\frac{\log_{10}T-5.5}{1.5}\right] \tag{3}$$

where $I=23.8$ eV is the ionization energy and $T_r(X)$ are Chebyshev polynomials.

As noted in [24], one can avoid explicitly evaluating [25] the Chevyshev polynomials by using Clenshaw's algorithm:

$$b_{n+2}=b_{n+1}=0\ ,$$

$$b_r=2Xb_{r+1}-b_{r+2}+a_r, \quad r=n,n-1,\ldots,0$$

$$\alpha(T)=\tfrac{1}{2}T^{1/2}e^{-I/kT}(b_0-b_2)\ .$$

ACKNOWLEDGMENTS

This work was supported in part by the Office of Fusion Energy of the U.S. Department of Energy under Contract No. DEA105-86ER53237 with the National Institute of Standards and Technology. E. D. was supported by the NSF Research Experience for Undergraduates Program. We are grateful to C. V. Kunasz for helping us with the rate coefficient fit.

*Permanent address: Institute of Physics, P.O. Box 57, 11001 Beograd, Yugoslavia.

†Present address: Physics Department, Rice University, Houston, TX 77251.

‡Quantum Physics Division, National Institute of Standards and Technology.

[1] For a review, see G. H. Dunn, in *Electron Impact Ionization,* edited by T. D. Märk and G. H. Dunn (Springer-Verlag, New York, 1985), p. 277.

[2] For a review, see S. M. Younger, in *Electron Impact Ionization,* edited by T. D. Märk and G. H. Dunn (Springer-Verlag, New York, 1985), p. 1.

[3] R. K. Janev, M. F. A. Harrison, and H. W. Drawin, Nucl. Fusion **29**, 109 (1989).

[4] D. W. Mueller, T. J. Morgan, G. H. Dunn, D. C. Gregory, and D. H. Crandall, Phys. Rev. A **31**, 2905 (1985).

[5] I. Yamada, A. Danjo, T. Hirayama, A. Matsumoto, S. Ohtani, H. Suzuki, T. Takayanagi, H. Tawara, K. Wakiya, and M. Yoshino, J. Phys. Soc. Jpn. **58**, 3151 (1989).

[6] W. T. Rogers, G. Stefani, R. Camillioni, G. H. Dunn, A. Z. Msezane, and R. J. W. Henry, Phys. Rev. A **25**, 737 (1982).

[7] M. Menzinger and L. Wahlin, Rev. Sci. Instrum. **40**, 102 (1969).

[8] Johnston Laboratories, Model No. MM-1. This information is provided for technical completeness and not as a

product endorsement.
[9] P. O. Taylor and G. H. Dunn, Phys. Rev. A **8**, 2304 (1973).
[10] P. O. Taylor, K. T. Dolder, W. E. Kauppila, and G. H. Dunn, Rev. Sci. Instrum. **45**, 538 (1974).
[11] K. T. Dolder and B. Peart, Rep. Prog. Phys. **39**, 693 (1976).
[12] W. T. Rogers, Ph.D. thesis, University of Colorado, 1980 (unpublished, available through University Microfilms, Ann Arbor, MI).
[13] G. H. Dunn, in *Atomic Physics,* edited by B. Bederson, V. W. Cohen, and F. M. J. Pichanick (Plenum, New York, 1969), p. 417.
[14] K. T. Dolder, in *Case Studies in Atomic Collision Physics,* edited by E. W. McDaniel and M. R. C. McDowell (North-Holland, Amsterdam, 1969), Vol. 1, p. 249.
[15] C. E. Moore, Atomic Energy Levels, Natl. Bur. Stand. (U.S.) Circ. No. 467 (U.S. GPO, Washington, DC, 1949), Vol. 1.
[16] Cary Model No. 31 with a 10^{12}-Ω input resistor. This device was calibrated to within 1% after the measurements. The manufacturer and model number are given for technical completeness and not as an endorsement of a product.
[17] A. Müller, K. Huber, K. Tinschert, R. Becker, and E. Salzborn, J. Phys. B **18**, 2993 (1985).
[18] K. F. Mann, A. C. H. Smith, and M. F. A. Harrison, J. Phys. B **20**, 5865 (1987).
[19] W. Lotz, Z. Phys. **216**, 241 (1968).
[20] D. L. Ziegler, J. H. Newman, L. N. Goeller, K. A. Smith, and R. F. Stebbings, Planet. Space Sci. **30**, 1269 (1982).
[21] R. S. Freund, R. C. Wetzel, R. J. Shul, and T. R. Hayes, Phys. Rev. A **41**, 3575 (1990).
[22] M. A. Lennon, K. L. Bell, H. B. Gilbody, J. G. Hughes, A. E. Kingston, M. J. Murray, and F. J. Smith, J. Phys. Chem. Ref. Data **17**, 1288 (1988). This paper is a compendium of evalauated and recommended data.
[23] E. Clementi and C. Roetti, At. Data Nucl. Data Tables **14**, 177 (1974).
[24] D. H. Crandall, G. H. Dunn, A. Gallagher, D. G. Hummer, C. V. Kunasz, D. Leep, and P. O. Taylor, Astrophys. J. **191**, 789 (1974).
[25] Since a_8 is the last coefficient given, start with b_8, noting that $b_9 = b_{10} = 0$; then proceed to b_7 and so on.